Supporting online materials

Developing next generation matrices from existing data

The estimates of transmission rates in each sector (i.e., home, school, work and other locations) and the overall reproduction number are derived from baseline estimates of the daily, age-specific contact rates between individuals of different age groups. These contact rates are provided by the analysis in *Prem et al*.(1) where data from population-based contact diaries in eight European countries were projected to generate contact intensities for 144 other countries using Bayesian modelling techniques. The inferred values $c_{aa'}$ give the number of (pre-COVID-19) typical daily contacts an individual of age a' makes with an individual of age a. In the dataset, age bands are separated into 5 year age groups and contacts are further divided into four locations: work, home, school and other.

To estimate the transmission capacity associated with these contacts we convert the contact intensity matrices to next-generation matrices, K, whose elements, $k_{aa'}$, give the number of new infections of age a generated by individuals of age a'. As a first step, we compute an unscaled next-generation matrix $\overline{K}$ by weighting the elements of the contact matrix $c_{aa'}$ by the age-dependent relative susceptibility (σ_a) and infectivity (β_a) of individuals in the population and the distribution of susceptible (s_a) and total (n_a) individuals in each age group. In particular, the elements, $\bar{k}_{aa'}$, of the unscaled next-generation matrix (NGM), $\overline{K}$, are given by

$$\bar{k}_{aa'} = \frac{\sigma_a s_a c_{aa'} \beta_{a'}}{n_{a'}}.$$

Here σ_a is the relative susceptibility to infection for an individual in age group a and β_a is their corresponding transmissibility once infected. Since the population is entirely susceptible upon first introduction of the infection such that $s_a = n_a$.

For symmetry, we assume that the age-dependent susceptibility and transmissibility profiles are equal equivalent, i.e., $\sigma_a = \beta_a$, and are given by the following parametric equation:

$$\sigma_a = \frac{1 - \sigma_{\text{rel}}}{2} \tanh(b(a - c)) + \frac{1 + \sigma_{\text{rel}}}{2}$$

where σ_{rel} is approximately equal to the relative susceptibility between individuals in the youngest (<5) and those in the oldest (>80) age groups. In the following analysis we assume baseline values of $\sigma_{\min}$ = 0.1, b = 0.3 and c = 27.

We choose values to match the proportion of each age group infected in China (the country used to calibrate the model) and then applied the calibrated values to Australian mixing matrices.

Figure 1 shows the calibrated normalized eigenvector fo the NGM, reflecting the model-estimated age distribution of infected people (compared with observed values in China(2)). This assumes that the age-case distribution reflects the age-infection distribution; that is that the clinical fraction is unchanged by age (this assumption is explored further in work by Davies *et al*. (3)). We relax this assumption in the sensitivity and uncertainty analyses.

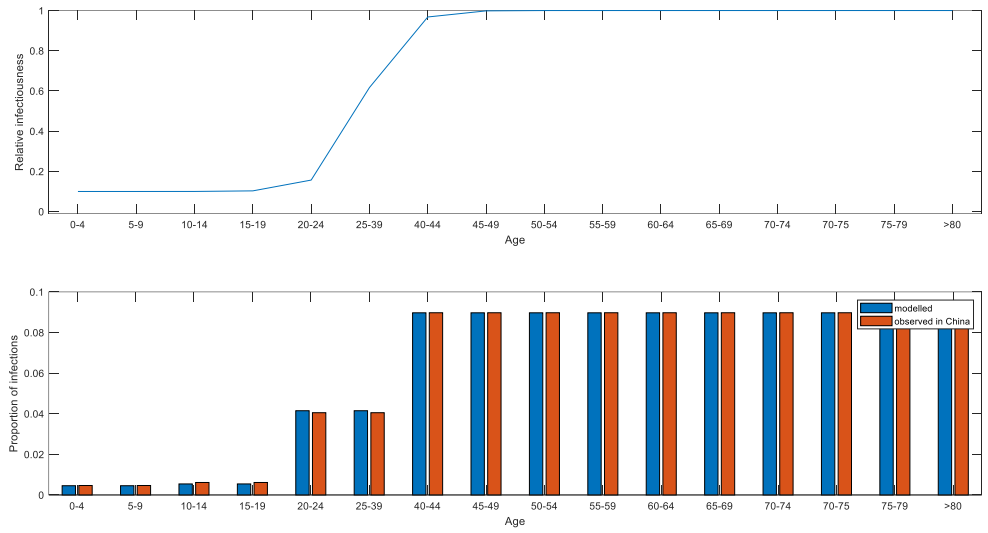

Figure 1. Fitted relative infectiousness profile (top panel) and values for age distribution, modelled and observed for China (2) (bottom panel).

The unscaled next-generation matrix $\overline{K}$ is converted into the true next-generation matrix K through the scaling factor η:

$$K = \eta\overline{K}$$

where η can be thought of as the average lifetime transmission rate per contact of each infectious individual. Note that any normalization factors generated by setting $\sigma_a = \beta_a$ (rather than $\sigma_a \propto \beta_a$) can in principle be absorbed into the scaling factor η.

The basic reproduction number is the maximal eigenvalue of the NGM:

$$R_0 = \rho(K) = \eta\rho(\overline{K})$$

where $\rho(\cdot)$ denotes the spectral radius. We can arrange this equation to obtain an expression for the scaling factor η:

$$\eta = \frac{R_0}{\rho(\overline{K})}.$$

Substituting the estimated basic reproduction number in China R_0 = 2.68 (95% crI: 2.47 – 2.86) yields η = 0.27.

The scaling factor η could be written as

$$\eta = \int_0^\infty \gamma(\tau) f(\tau)\, d\tau,$$

where $\gamma(\tau)$ is the probability of transmission per contact per unit time for an individual who has been infected for τ units of time and $f(\tau)$ is the corresponding probability that they remain infected.

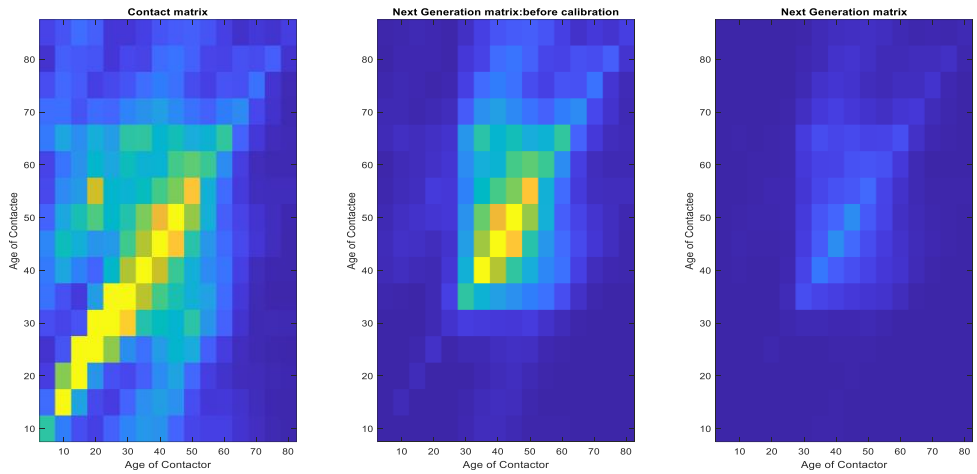

Figure 2. A comparison between the contact matrix and the next generation matrix for China. Left panel is the contact matrix for China taken from Prem et al.(1) Middle column is the matrix following changes made to relative infectiousness and relative susceptibility by age. Right panel is the final calibrated next generation matrix for China of 2.68(4).

We then applied these calibration values to a new contact matrix for Australia based on Prem *et al.(1)* to arrive at Australian R_0, by using the calibrated values for η, σ, b, c. This results in a derived R_0 of 2.49.

We then used google results for reduction in position of people at the various locations (cite google) and results from Victorian Education Department (cite this), to derive a table of relative macro changes in locations during the lockdown of 0.66 for other, 1.18 for home, 0.6 for workplaces and 0.03 for school.

Including all of these macro-distancing measures leads to an R_{eff} = 1.76. To adjust all activities outside the home by allowing for micro-distancing at locations: other, school and workplace, leads to a *micro-distancing* factor of 0.26. That is, the rules and change in behavior regarding physical distancing at locations is estimated to reduce the probability of infectious contact to 26% of that priror to these steps being taken, while the decision to remain at home, not attend other locations is estimated to reduce infectious contacts to 1.76/2.49, or 71% of previous levels.

The matrices provided by Prem *et al.(1)* are synthetic and estimated based on a number of features in Australia including school attendance, workplace size and so one. While this is a potential weakness, we believe these are the most complete contact matrices available in Australia.

Table 1. Parameters in the model.

Parameter	Value	Explanation
Baseline and Macro-distancing measures		
Reproduction number	R_{eff}	Typical number of secondary infections per infected person
China: early pandemic	2.68	
Business as usual Australia	2.49	Reproduction number in the absence of interventions, using value for China calibrated to Australian mixing patterns
Mixing distribution	Taken from study applied to Australian population	Prem *et al.(1)*
Change in mixing during school closure School-based mixing multiplier	0.03	Schools not open to students, except for very few (~3%) who then undertake physical distancing and online learning, with no sport or face-to-face lessons(5)
Work-based mixing multiplier	0.66	Google Mobility Report(6)
Other	0.6	Google Mobility Report (6)
Home	1.18	Google Mobility Report (6)
Scenario: Current Lockdown, *micro-distancing* and public health response		
Change in mixing during school closure School-based mixing multiplier	0.03	(5)
Work-based mixing multiplier	0.66	(6)
Other	0.6	(6)
Home	1.18	(6)
Micro-distancing and public health response	0.26	The above measures bring lockdown R_{eff} to 1.78. Multiplying contacts at school, home and other by 0.26 brings the lockdown R_{eff} to 0.80
Scenario: Current Lockdown & Open Schools		
Change in mixing during school closure School-based mixing multiplier	1	Schools reopen with increased distancing measures put into place in the staffroom.
Work-based mixing multiplier	0.66	(6)
Other	0.6	(6)
Home	1.18	(6)
Remove home lockdown, return to school educate community on physical distancing		
Change in mixing during school closure School-based mixing multiplier	1	Schools open to students and staff undertake physical distancing

Work-based mixing multiplier	0.66	(6)
Other	1	No home lockdown, but reduced social congregation and limited gatherings
Home	1.09	Many adults continue to work from home but children are now at school so the effect of increased home intensity of contacts is assumed to be halved.
Remove home lockdown, return to school and work educate community on physical distancing and continue vigorous testing and quarantine		
Change in mixing during school closure School-based mixing multiplier	1	All macro-distancing returns to normal
Work-based mixing multiplier	1	All macro-distancing returns to normal
Other	1	All macro-distancing returns to normal
Home	1	All macro-distancing returns to normal
Micro-distancing and public health response	0.26	As above

Sensitivity analysis: children account for 10% of infectiousness not 2%

Because it is one of the strongest assumptions in this work and potentially highly influential, we examine the sensitivity of our results to the assumption that the clinical fraction of cases found in those under 20 years of age is reflected in the infectiousness of this age group. That is, our baseline assumption is that the 2% of cases identified as under 20 reflects 2% infectious cases in this age group. If however, asymptomatic cases are more frequent in this age group and are also infectious, this assumption may be incorrect and influential in the results. We therefore explore the possibility that children may account for up to 10% of infections and be infectious despite not being included as cases, in our sensitivity analysis. Figure 3 shows the resulting distribution of proportion of the infections and relative infectiousness and susceptibility. Calibrating to allow 10% of infections to be in children <20 years, leads to a value of 0.5 relative susceptibility and infectiousness. This is equivalent to suggesting that children are 5 times more likely to be undiagnosed - asymptomatic - than adults and overall two times less infectious/susceptible.

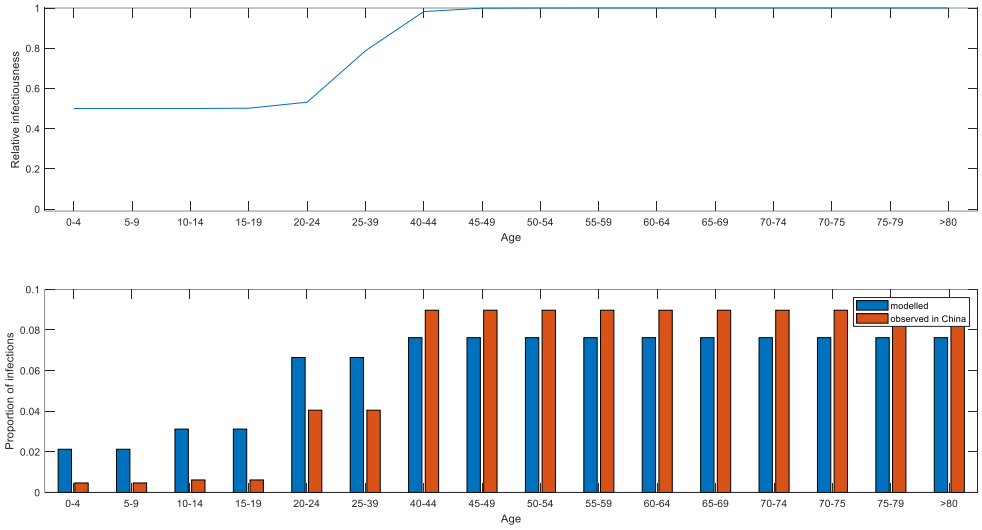

Figure 3. Calibrating the infectiousness and susceptibility of children to fit the assumption that children under 20 years make up 10 percent of infections rather than 2%. This is equivalent to assuming for every case in children there are four additional cases that are asymptomatic, and these cases are just as infectious as symptomatic people in the same age group.

The sensitivity analysis requires recalibration of values for $\eta, \sigma, \mathrm{b}, \mathrm{c}$, to fit the data, with values of η =1/4.072, $\sigma = 0.5, b = 0.3$ and $c = 27$. This means that the calibrated value to allow for 10% of infections to be children is 0.5 -that is children are half as infectious and susceptible as adults. Then new next generation matrices for Australia are determined and the micro-distancing factor is reset to 0.21 to achieve R_{eff} = 0.8.

Finally, the impact of school closure/opening and other activities is reassessed, as shown in Figure 4 below. These results show that our broad conclusions are robust to assumptions about child infectiousness. Reduction in R_{eff} is driven principally by *micro-distancing* at locations where transmission may occur rather than avoidance of these places.

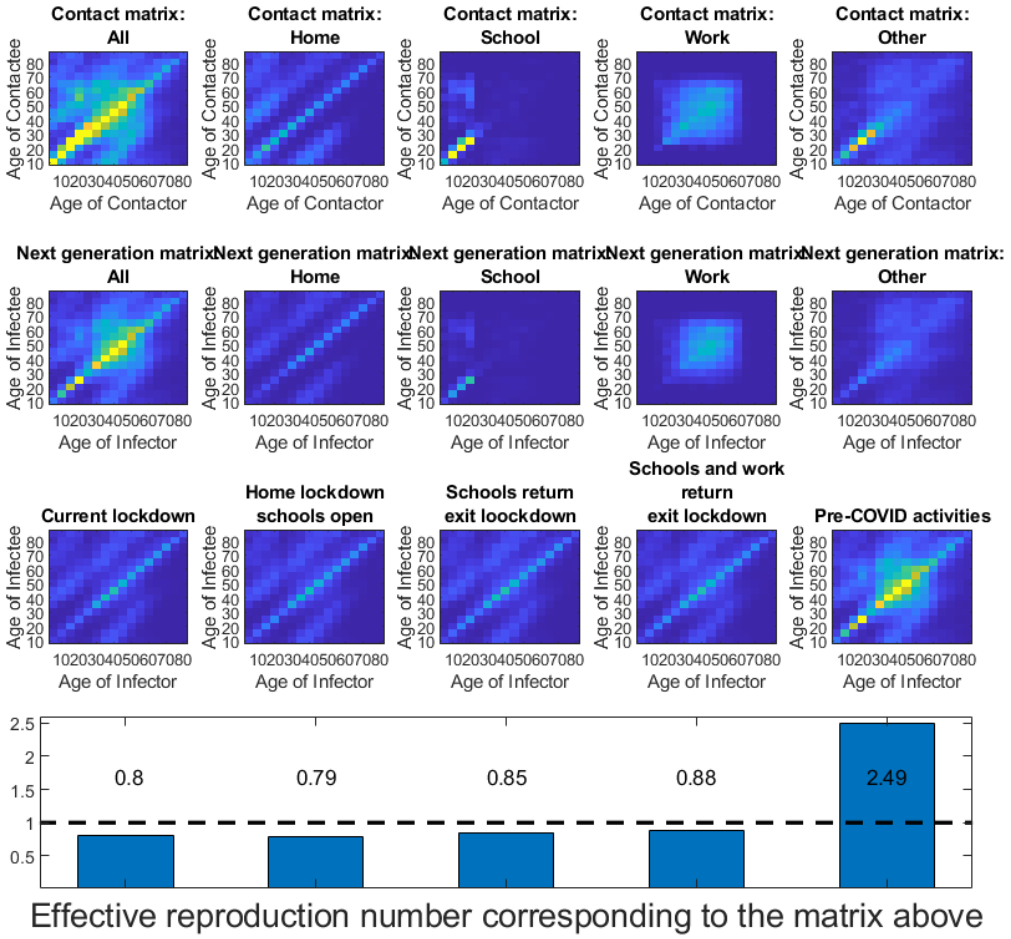

Figure 4. Top row contact matrices, second row, next generation matrices by location and third row next generation matrices according to exit strategy in Australia and associated effective reproduction number (bottom row) under the assumption that 10% of infections are in children under 20 years and that these children have 50% infectiousness and susceptibility compared with adults.

Sensitivity Matrices

Caswell(7) shows that the change in the total reproduction number, for each element of the next generation matrix $\frac{\partial R_0}{\partial a_{ij}}$, is given by the outer product of the right and left Eigenvalues (row vectors w and v), normalized by their dot product $\frac{\mathrm{w'v}}{\mathrm{v'w}}$.

Figure 5 shows the resulting sensitivity matrix for the base case next generation matrix for Australia. In the baseline case, contacts between adults aged 30 to 50 are the most important contributers to the overall population reproduction number. Relaxing assumptions about the susceptibility and infectiousness of the under 20s reduces the importance of the 30-50 age group and increasing the importance of all age groups as infectors.

Figure 5. Sensitivity matrices of R_{eff} to the next generation matrix under four different susceptibility and infectiousness assumptions. Baseline is infectiousness and susceptibility of children under 20 years being 10%, top right shows the assumption that children are equally susceptible but 10% as infectious, bottom left is the assumption that under 20s are 50% as infectious and 50% susceptible and account for 20% of all infections. Bottom right assumes under 20s are 50% as infectious and 100% as susceptible as over 20s.

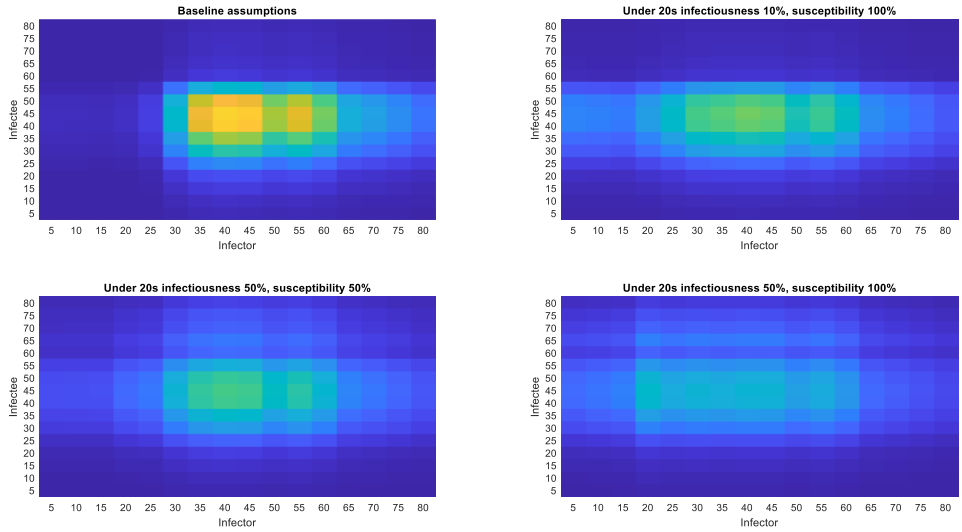

Full sensitivity and uncertainty analysis

We examined the impact of changing the main estimated parameters of the model across a range of values shown in Table 2. The impact on the model outcome was determined by Monte Carlo Markov Chain (MCMC) sampling from a prior (uniform) distribution in that range. Seven outcomes were assessed. The major outcomes of R_0 and R_{eff} under lockdown were highly sensitive to most model parameters, as shown in Figures 6 and 7.

Table 3. Parameter values in the model, baseline and range of parameter exploration in the sensitivity and uncertainty analysis.

Parameter	Baseline	Lower	Upper
Overall calibration factor (allows R_0 to be increased and decreased)	0.27	0.2 Parameters are drawn from prior distribution uniform [2,5] and then the reciprocal is taken	0.5
Child infectiousness	0.1	0.05	1
Child susceptibility	0.1	0.05	1
Micro-distancing factor: school	0.21	0.05	1
Micro-distancing factor: work	0.21	0.05	1
Micro-distancing factor: other	0.21	0.05	1

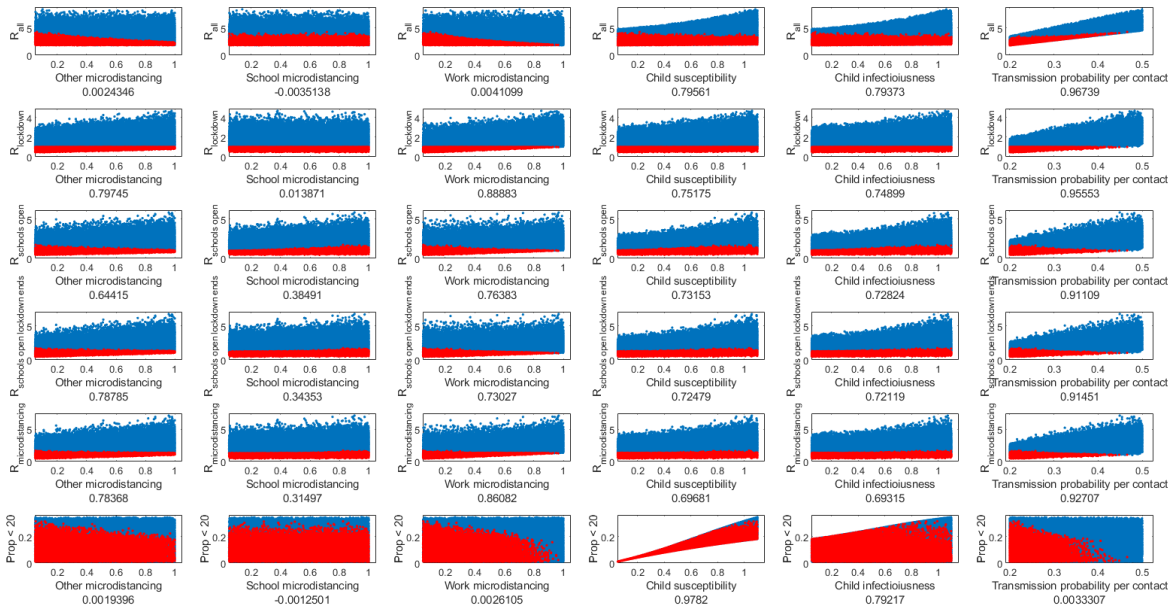

Figure 6. MCMC results using prior distributions for parameters given in Table 3 above. The values for which the R_{eff} is <1 for the full lockdown are shown in red. The partial correlation is provided for each parameter/outcome pair.

Figure 7. Sensitivity analysis plots of sensitivity of important model outcomes to the parameters used in the model.

Results of figure 7 show that the model outputs are highly sensitivity to the model inputs and therefore conclusions must be made with caution. However, it is notable that the model parameter to which outcomes are least sensitive is the value of school distancing.

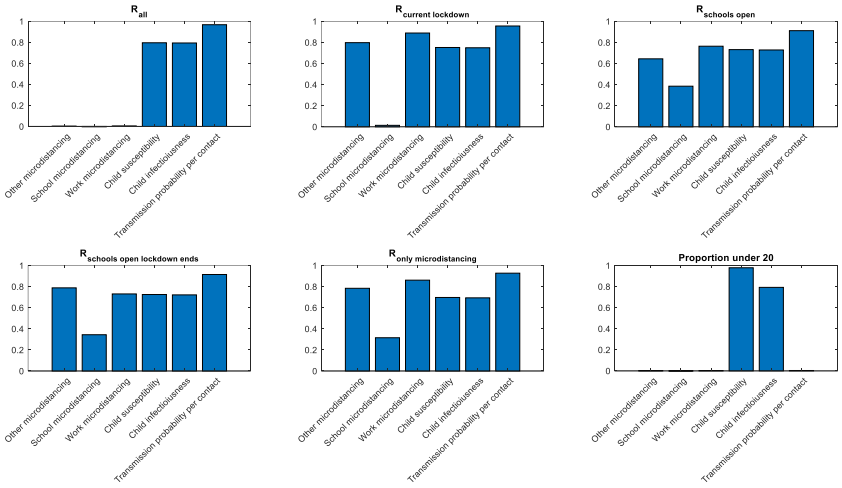

Uncertainty analysis

From the MCMC we used a variation of the Approximate Bayesian computation method to choosing only elements in the chain in which the current lockdown R_{eff} is less than one.

The resulting posterior values for the parameters and the other outcomes are shown in figure 8. This suggests that knowing that Australia achieved an effective reproduction number below one during the lockdown provides some information for estimating the uncertain parameters. In particular, micro-distancing at *work* and *other* locations is estimated to be much more effective in the posterior distribution (this is a multiplying factor so the smaller the number the higher the impact). The posterior values for child infectiousness and susceptibility of approximately 0.1 that of adults in line with expectations (precise maximum *a posteriori* values are 0.15 for susceptibility and 0.08 for infectiousness). The posterior values are also helpful for estimating the impact of school and workplace opening. The 95% credible interval is used to provide error bars for Figure 1 of the main text.

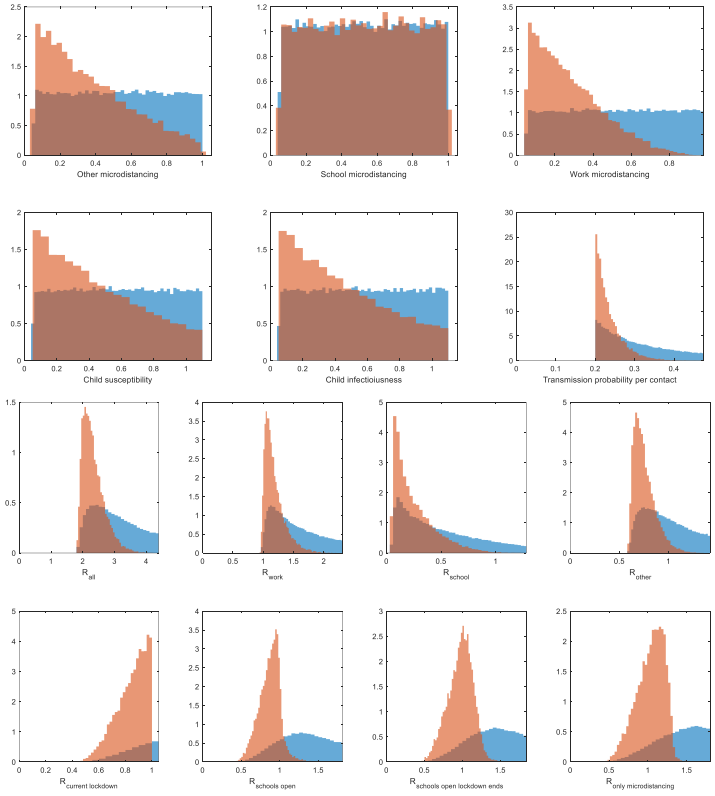

Figure 8. Posterior (brown) and prior (blue) probability density functions from the uncertainty analysis, using an Approximate Bayesian Computation rejection method, selecting only results with $R_{\text{current lockdown}}<1$.

References

1. Prem K, Cook AR, Jit M. Projecting social contact matrices in 152 countries using contact surveys and demographic data. PLoS Comput Biol. 2017;13(9):e1005697.
2. Wu Z, McGoogan JM. Characteristics of and Important Lessons From the Coronavirus Disease 2019 (COVID-19) Outbreak in China: Summary of a Report of 72314 Cases From the Chinese Center for Disease Control and Prevention. JAMA. 2020.
3. Davies NG, Klepac P, Liu Y, Prem K, Jit M, Eggo RM, et al. Age-dependent effects in the transmission and control of COVID-19 epidemics. medRxiv. 2020.
4. Liu Y, Gayle AA, Wilder-Smith A, Rocklov J. The reproductive number of COVID-19 is higher compared to SARS coronavirus. J Travel Med. 2020.
5. The_Age:. Merlino says just 3% of students went to school on first day of term 2020 [
6. Google. COVID-19 Community Mobility Report 2020 [
7. Caswell H. Matrix population models : construction, analysis, and interpretation. Sunderland, Mass.: Sinauer Associates; 1989. xiv, 328 p p.